Submitted to the International Europhysics Conference on High Energy Physics EPS-HEP99
Tampere, Finland, 15-21 July 1999

Determination of the Strong Coupling Constant from the Inclusive Jet Cross Section in Deep-Inelastic Positron-Proton Collisions at HERA

H1 Collaboration

Abstract

We have measured the inclusive jet cross section in the Breit frame in deep-inelastic scattering at large four momentum transfers squared Q^2 and large transverse jet energies E_T using the inclusive $k_\perp$ jet algorithm. The analysis is based on data corresponding to an integrated luminosity of $\mathcal{L} \simeq 33\,\mathrm{pb}^{-1}$ taken in the years 1995-1997 with the H1 detector at the positron-proton collider HERA at a center-of-mass energy $\sqrt{s}_{ep} = 300\,\mathrm{GeV}$. The inclusive jet cross section is presented double differentially as a function of E_T and Q^2 in the range $49 < E_T^2 < 2500\,\mathrm{GeV}^2$ and $150 < Q^2 < 5000\,\mathrm{GeV}^2$. In a QCD analysis of the data we have determined the strong coupling constant α_s. Setting the renormalization scale equal to the transverse jet energy, we investigate the running of $\alpha_s(E_T)$. We present comprehensive studies of the dependence of the results on the parton distributions used in the fit. Finally we have performed a combined fit to the data over the whole range of E_T and Q^2 and obtain a preliminary result of $\alpha_s(M_Z) = 0.1181 \pm 0.0030(\mathrm{exp})^{+0.0039}_{-0.0046}(\mathrm{theo})^{+0.0036}_{-0.0015}$(parton density functions). We have repeated the analysis setting the renormalization scale to the four momentum transfer $\mu_r = Q$ and obtain a preliminary result of $\alpha_s(M_Z) = 0.1221 \pm 0.0034(\mathrm{exp.})\,^{+0.0054}_{-0.0059}(\mathrm{theo.})\,^{+0.0033}_{-0.0016}(\mathrm{pdf})$ with an increased theoretical uncertainty resulting from a larger renormalization scale dependence.

Abstract: 157
Parallel sessions: 1
Plenary sessions: 1

Electronic Access: http://www-h1.desy.de/publications/

1 Introduction

Jet production in deep-inelastic scattering at large transverse energies E_T in the Breit frame[1]can be used to test the predictions of QCD. When non-perturbative contributions are sufficiently small high E_T jet cross sections are directly sensitive the strong coupling constant α_s. Two large energy scales are characteristic for this process: the transverse jet energy in the Breit frame E_T and the four momentum transfer to the lepton Q. It is therefore of interest to study jet production as a function of both of these scales.

We present a measurement of the inclusive jet cross section in the Breit frame in neutral current deep-inelastic scattering at large four momentum transfers squared $150 < Q^2 < 5000\,\mathrm{GeV}^2$ and large transverse jet energies in the Breit frame $7 < E_T < 50\,\mathrm{GeV}$. The analysis is based on data taken in the years 1995-1997 with the H1 detector at the ep collider HERA at $\sqrt{s}_{ep} = 300\,\mathrm{GeV}$, corresponding to an integrated luminosity of $\mathcal{L} \simeq 33\,\mathrm{pb}^{-1}$. The jets are defined by the inclusive $k_\perp$ algorithm [1, 2] which has been seen to have smaller hadronization corrections than other jet algorithms [3].

In a subsequent QCD analysis we determine the strong coupling constant α_s from the inclusive jet cross sections. We study the running of α_s as a function of E_T which is used as the renormalization scale $\mu_r = E_T$. We also discuss the α_s results for an alternative choice of $\mu_r = Q$. In a comprehensive study we test the dependence of the result on the parton distributions used in the QCD analysis.

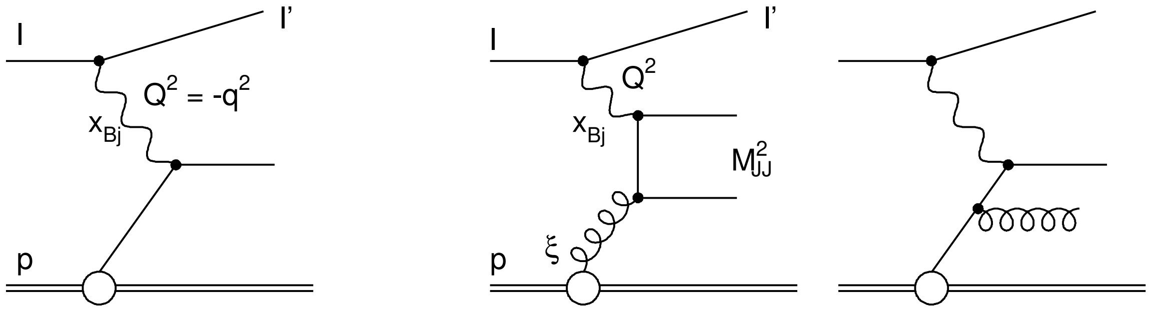

Figure 1: Feynman diagrams of different processes in deep-inelastic lepton proton scattering: The Born process (left), boson-gluon fusion (middle) and the QCD-Compton process (right).

In the HERA laboratory frame high E_T jets are predominantly produced in electroweak Born processes[2] as sketched in the left diagram in Fig.1 and their transverse energy is mainly a reflection of the kinematics of the scattered lepton. The production of events with higher jet multiplicities in boson-gluon fusion or QCD-Compton processes (Fig.1, middle and right diagram) is only a relatively small modification of this picture. The analysis of hard QCD processes, when performed in the HERA laboratory frame, requires therefore the selection of events with multi-jet structures in the hadronic final state. Dijet systems can for example be resolved by invariant mass criteria, as applied in the definition of the modified JADE algorithm [4, 5]. In previous publications we have presented QCD analyses based on this method [6, 7].

[1]"transverse" refers to the z-axis which is given by the axis of the virtual photon and the proton.
[2]The term "jets" refers here only to hadronic activity well-separated from the proton remnant.

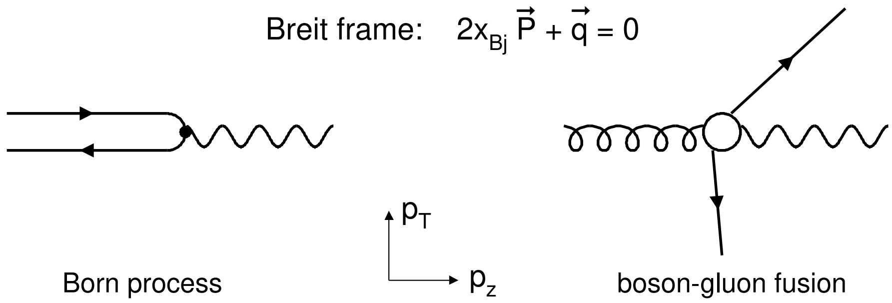

Figure 2: Deep-inelastic scattering in the Breit frame: in the Born process at $\mathcal{O}(\alpha_s^0)$ (left) and in boson-gluon fusion at $\mathcal{O}(\alpha_s)$ (right).

This situation is different in the Breit frame where the purely space-like gauge boson (γ/Z) with four momentum $q_{\gamma/Z} = \{0, 0, 0, -Q\}$ collides with a parton from the proton. In the Born process the incoming quark is back-scattered into the negative z direction (Fig. 2, left) and no transverse energy is produced. Only in hard QCD processes, as described in order $\mathcal{O}(\alpha_s)$ by the diagrams in Fig.1 (middle and right), the final state in the Breit frame contains jets of large transverse energy (Fig. 2, right). The high E_T inclusive jet cross section in the Breit frame receives no contributions from the Born process and is therefore directly sensitive to the strong coupling constant α_s.

2 Data and Selection and Correction Procedure

The data used in this analysis were collected during the years 1995 to 1997 using the H1 detector [8] at the HERA collider which was operated with positrons at an energy of $E_e = 27.5\,\text{GeV}$ and protons at $E_p = 820\,\text{GeV}$.

2.1 Selection of Neutral Current DIS Events

The data selection follows closely the one used in a recent measurement of the inclusive ep cross section at high Q^2 [9]. The scattered positron is identified as a localized electromagnetic energy deposit in the Liquid Argon (LAr) calorimeter ($4^\circ < \theta < 154^\circ$)[3] with large transverse momentum. The hadronic final state is reconstructed from a combination of low momentum tracks ($p_T < 2\,\text{GeV}$) and energy deposits measured in the LAr calorimeter and in the backward calorimeter (SPACAL, $154^\circ < \theta < 177.8^\circ$).

The event kinematics is determined from a redundant set of variables from the scattered positron and the hadronic final state. These are the polar angle θ_e and the energy E'_e of the scattered positron and the variable Σ which is defined as $\Sigma \equiv \sum_h (E_h - p_{z,h})$, where the sum runs over all particles h of the hadronic final state[4]. The kinematic variables are then

[3]The polar angle θ is defined with respect to the proton direction.

[4]"particle" refers to all hadronic final state objects (excluding the scattered positron) whether these are tracks or calorimetric energy clusters.

reconstructed by the so-called “Electron-Sigma” method [10], which is a combination of the Electron method [11] and the Sigma method [12]

$$Q^2_{e\Sigma} = 4E_e E'_e \cos^2\frac{\theta_e}{2}\,, \qquad x_{e\Sigma} = \frac{E'^2_e \sin^2\theta_e}{s\, y_\Sigma(1-y_\Sigma)}\,, \qquad y_{e\Sigma} = \frac{2E_e}{\Sigma + E'_e(1-\cos\theta_e)} y_\Sigma\,,$$

with

$$y_\Sigma = \frac{\Sigma}{\Sigma + E'_e(1-\cos\theta_e)}\,.$$

The phase space for the present analysis is given by

$$150 < Q^2 < 5000\,\text{GeV}^2\,, \qquad 0.2 < y < 0.6\,.$$

2.2 Jet Selection

After the scattered positron is excluded all hadronic final state particles are boosted to the Breit frame which is defined by $\vec{q} + 2x_{Bj}\vec{P} = 0$ where $\vec{P}$ is the momentum of the incoming proton and $\vec{q}$ is the momentum from the exchanged boson. Jets are defined by the inclusive $k_\perp$ cluster algorithm [1, 2] which is applied to all hadronic final state particles in the Breit frame. Jets are selected when their transverse energies in the Breit frame E_T and their pseudorapidities[5] in the HERA laboratory frame $\eta_{\text{jet,lab}}$ fulfill

$$E_T > 7\,\text{GeV}\,, \qquad -1 < \eta_{\text{jet,lab}} < 2.5\,.$$

The inclusive jet cross section is measured double differentially in four regions of E_T and in four regions of Q^2.

2.3 Correction of the Data

The data are corrected in a bin-by-bin correction procedure for detector effects and for QED radiation. The correction factors are determined using events generated by the event generators LEPTO [13] and ARIADNE [14] (both interfaced by DJANGO [15]) that were subjected to a detailed simulation of the H1 detector. These simulated events give a good description of the properties of the hadronic final state. Although they fail to describe the absolute normalization of inclusive jet distributions, the shapes of the transverse energy spectra and of the angular jet distributions are reasonably well described. This is also the case for single jet properties as jet shapes and subjet multiplicities.

2.4 Experimental Uncertainties

All experimental uncertainties are grouped into two classes: uncertainties which are correlated between the data points and uncorrelated ones.

[5]The pseudorapidity η is defined as $\eta \equiv -\ln(\tan\theta/2)$ where θ is the polar angle with respect to the proton direction.

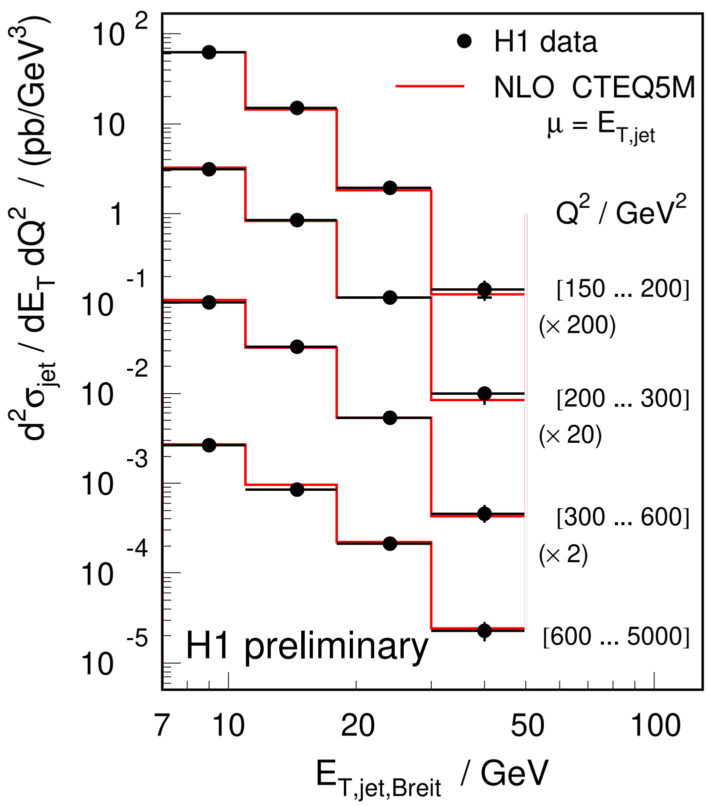

Figure 3: The inclusive jet cross section as a function of the transverse jet energy in the Breit frame E_T in different regions of the four momentum transfer squared Q^2. The data are compared to the predictions of a next-to-leading order calculation by the program DISENT.

Correlated experimental uncertainties are the model dependence of the detector and radiative correction (given by the spread of the two models estimates), uncertainties of the hadronic energy scale ($\pm 4\%$ from which $\pm 2\%$ are correlated) the electromagnetic energy scale (between $\pm 0.7\%$ and $\pm 3\%$, depending on θ_e, from which 0.5% are correlated), and uncertainties from the determination of the luminosity ($\pm 1.5\%$).

Uncorrelated experimental uncertainties are the statistical errors of the data and those of the correction factors and the uncertainties from the measurement of the track momenta (varied by $\pm 3\%$), and from the hadronic energy measurement in the SPACAL (varied by $\pm 7\%$).

3 The Inclusive Jet Cross Section

The inclusive jet cross section is shown in Fig. 3 in the range of $150 < Q^2 < 5000\,\mathrm{GeV}^2$ and $7 < E_T < 50\,\mathrm{GeV}$. With increasing Q^2 we observe a slightly harder E_T spectrum. The data are compared to the predictions of perturbative QCD in next-to-leading order (NLO) as implemented in the program DISENT [16]. These predictions are obtained for CTEQ5M parton distributions [17] for a value of $\alpha_s(M_Z) = 0.118$ and a renormalization scale $\mu_r = E_T$. The factorization scale was set to a fixed value of the order of the average transverse jet energies $\mu_f = \sqrt{200}\,\mathrm{GeV} \simeq \langle E_T \rangle$. Over the whole range of E_T and Q^2 the NLO calculation gives a good description of the data.

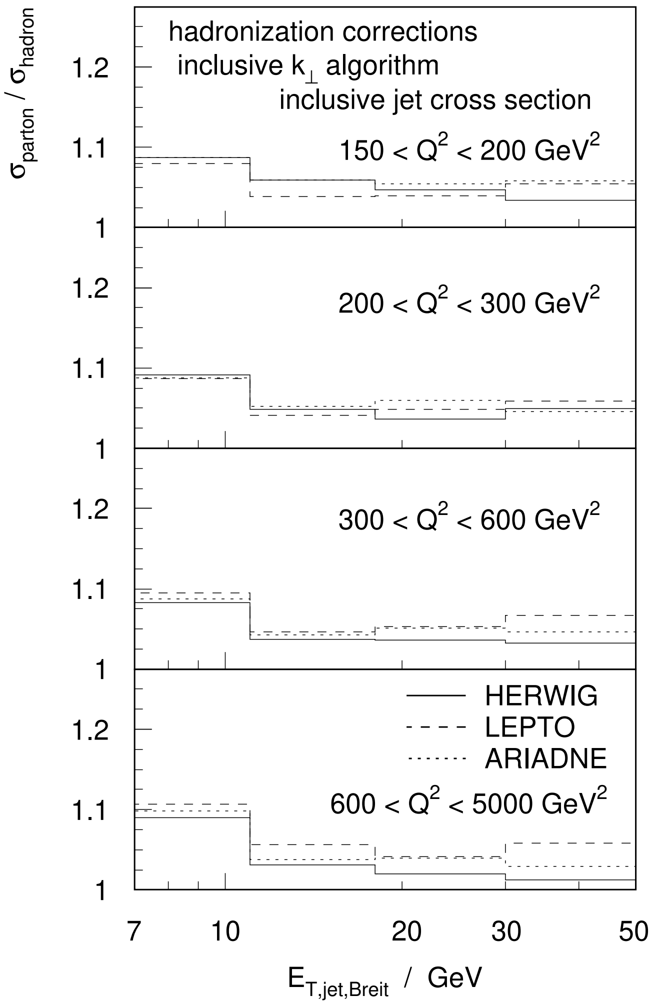

Figure 4: The hadronization corrections to the inclusive jet cross section, as predicted by the cluster fragmentation model (HERWIG) and the Lund String fragmentation model (LEPTO, ARIADNE). Shown is the ratio of the partonic jet cross section (i.e. before hadronization) and the hadronic jet cross section (i.e. after hadronization) as a function of E_T in different Q^2 ranges.

Hadronization Corrections

The direct comparison of a measured cross section (corrected for detector effects) with a purely perturbative calculation is only justified when non-perturbative contributions ("hadronization corrections") are small. The hadronization corrections are defined as the ratio of the jet cross sections before and after hadronization. Their size is estimated using the predictions of the HERWIG cluster hadronization model [18] and the Lund string fragmentation model [19] in JETSET [20]. These hadronization models are implemented in the event generators HERWIG [21], LEPTO [13] and ARIADNE [14] which include the $\mathcal{O}(\alpha_s)$ matrix elements combined with perturbative parton cascade models. In Fig. 4 we show the size of the hadronization corrections as predicted by these models. The hadronization corrections are seen to decrease with increasing E_T. It is seen that for the whole range covered in our analysis the hadronization corrections are reasonably small (between $3\% - 10\%$).

4 Sensitivity to α_s

In perturbative QCD the cross section of a deep-inelastic lepton proton scattering process can be written as a convolution of the perturbative coefficients c_a with the (non-perturbative) parton densities $f_{a/p}$ in the proton

$$\sigma_{\text{proc.}} = \sum_{a,n} \alpha_s^n(\mu_r^2) \int_0^1 d\xi \; c_{a,n}^{\text{proc.}}(\frac{x_{\text{Bj}}}{\xi}, \mu_r^2, \mu_f^2) \; f_{a/p}(\xi, \mu_f^2) \; . \tag{1}$$

The summation is performed over all contributing parton flavors a and all orders n of the strong coupling constant considered in the perturbative calculation. The integration is performed over all fractional parton momenta ξ. In the phase space region considered here the inclusive jet cross section is sensitive to the parton distributions at $0.007 \lesssim \xi \lesssim 0.4$.

The coefficients c_a are predicted by perturbative QCD. For the inclusive jet cross section in the Breit frame they are currently known to NLO [22]. The value of the strong coupling constant and the parton densities in the proton are not predicted by theory but enter the cross section formula as parameters which are universal, i.e. process independent.

This analysis is based on the assumption that the parton densities in the proton have been determined from global fits [17,23,24] to other data (i.e. structure function and Drell-Yan data). This assumption will be critically discussed later.

For given parton density functions the cross section in (1) depends only on a single free parameter: the strong coupling constant $\alpha_s(\mu_r)$ which depends on the value of the renormalization scale μ_r. The μ_r dependence of $\alpha_s(\mu_r)$ (i.e. the running) is predicted by perturbative QCD and is currently known to 4-loop accuracy [25,26].

Results for α_s are conventionally presented at a scale in the order of the typical process relevant energy scale. These α_s values can then be evolved to a common scale (usually the mass of the Z-boson M_Z) where they can be directly compared.

In jet production in deep-inelastic scattering there are two large energy scales. The transverse jet energy E_T is directly related to the jet-production vertex in the Feynman diagram and specifies the physical scale at which hard QCD radiation is resolved. Another large external momentum is given by the four momentum transfer Q. The present analysis will be performed for both choices $\mu_r = E_T$ and $\mu_r = Q$. To evolve the α_s values, determined at a scale $\mu_r = E_T$ (or $\mu_r = Q$) to $\mu_r = M_Z$ we use the exact numerical solution of the 4-loop renormalization group equation [26].

All NLO calculations are performed in the $\overline{\text{MS}}$ scheme for five massless quark flavors using the DISENT [16] program. The central α_s fit result is obtained for parton distributions from the CTEQ5M parameterization. The CTEQ5M parton distributions give the best description of the most recent H1 high Q^2 structure function data [9]. At a later stage we will also compare the α_s results for different parton distributions obtained in recent global fits which have been performed after 1995.

5 Principle of the Fit

The determination of α_s for a single data point or for a combined set of data points is done in a fit of the theoretical predictions to the data. During the fit the calculation of the NLO cross sections has to be repeated many times. Since standard computations of NLO cross sections are time-consuming we use a method for a fast reevaluation of the NLO cross sections as described in [27] (a similar method has been proposed in [28]). The fits are performed by a χ^2 minimization using the MINUIT program [29]. The definition of χ^2 fully takes into account all correlations of systematic uncertainties between the data points (as described in [30]).

The inclusive jet cross section is compared to the product of the NLO prediction and the hadronization correction (as defined above).

$$\sigma_{H1}^{\text{jet}} \leftrightarrow \sigma_{NLO}^{\text{jet}}(\alpha_s) \cdot c_{\text{hadronization}}^{-1} \qquad \text{where} \qquad c_{\text{hadronization}} = \frac{\sigma_{\text{parton}}}{\sigma_{\text{hadron}}} \,. \tag{2}$$

The value of the hadronization correction is taken as the mean value of the LEPTO, ARIADNE and HERWIG predictions. Since the spread between these models is small, we assign an enlarged uncertainty to this estimate of half of the size of the value, but at least 3%. This is a conservative estimate which accounts for the range of uncertainties discussed in [3].

In addition to the correlated and uncorrelated experimental uncertainties (as described in section 2.4) the following correlated theoretical uncertainties are considered: the uncertainty of the hadronization corrections and the renormalization and the factorization scale dependence of the perturbative predictions. The theoretical uncertainty from the renormalization scale dependence is determined by varying the renormalization scale in the range $0.25\, E_T^2 < \mu_r^2 < 4\, E_T^2$ (respectively $0.25\, Q^2 < \mu_r^2 < 4\, Q^2$) around its default value. The factorization scale is always set to the average transverse energy of the total jet sample $\mu_{f,0}^2 = \langle E_T^2 \rangle \simeq 200\,\text{GeV}^2$. The uncertainty from the factorization scale dependence is estimated by varying the scale within the large range of $0.125\, \mu_{f,0}^2 < \mu_f^2 < 9\, \mu_{f,0}^2$. While the renormalization scale dependence will be one of the largest uncertainties of the final result, the uncertainty from the factorization scale dependence is negligible.

A further source of uncertainty is introduced by the uncertainty in the parton distributions. This uncertainty can not really be estimated as long as the global fits are not performed with a consistent error analysis. We can therefore only try to give some estimate for this uncertainty by repeating the analysis for parton distributions from different global fits, taking the largest spread as uncertainty. Such a study is described in section 6.4.

6 Determination of α_s

Once the data set is given and the statistical procedure is defined, it is straightforward to obtain the result(s) for α_s. All α_s fit results presented in the following contain all experimental and theoretical uncertainties as described above. The uncertainties of the parton distributions will be discussed later in section 6.4.

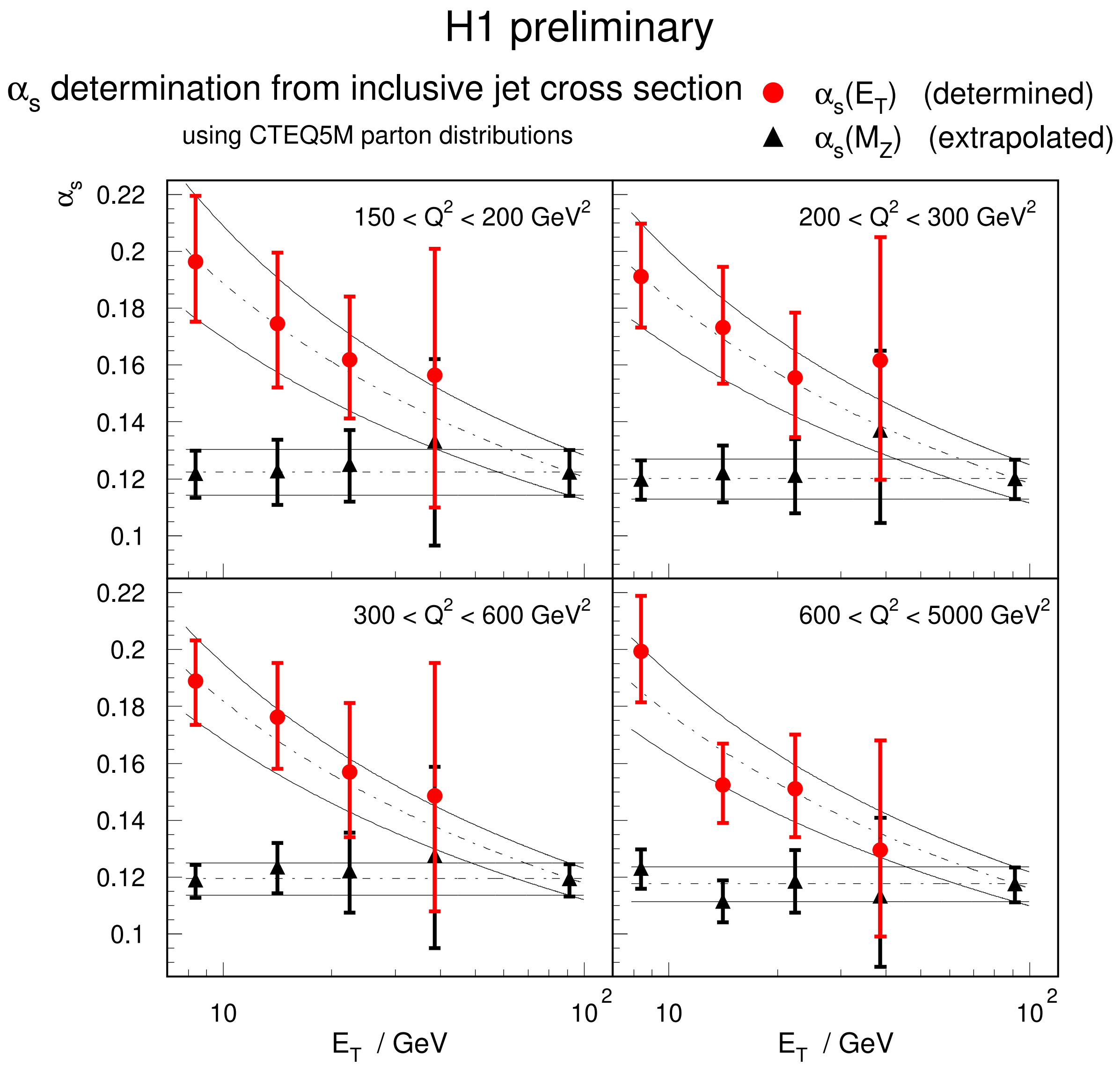

Figure 5: Determination of α_s from the inclusive jet cross section for $\mu_r = E_T$. Displayed are the results of the fits to the single data points in each Q^2 region at each E_T value (circles). The single values are extrapolated to the Z-mass (triangles), and a combined fit gives a result of $\alpha_s(M_Z)$ (rightmost triangle) for each Q^2 region. The upper curves indicate the prediction of the renormalization group equation for the combined fit results and their uncertainties.

6.1 Single Fits

We start to perform an α_s fit to each single data point, as shown in Fig. 5. For each data point we determine a corresponding value of $\alpha_s(E_T)$ (circles) which is presented at the average E_T of the corresponding data point. The single results are subsequently evolved to $\alpha_s(M_Z)$ (triangles below). Furthermore a combined fit to all data within the single Q^2 regions is performed, leading to a combined result of $\alpha_s(M_Z)$ for each Q^2 region (rightmost triangle). The upper curves in the plots indicate the prediction of the renormalization group equation for the combined results and their uncertainties. We see that all the single $\alpha_s(E_T)$ values are consistent with the predicted running. Furthermore all combined $\alpha_s(M_Z)$ results are compatible with each other.

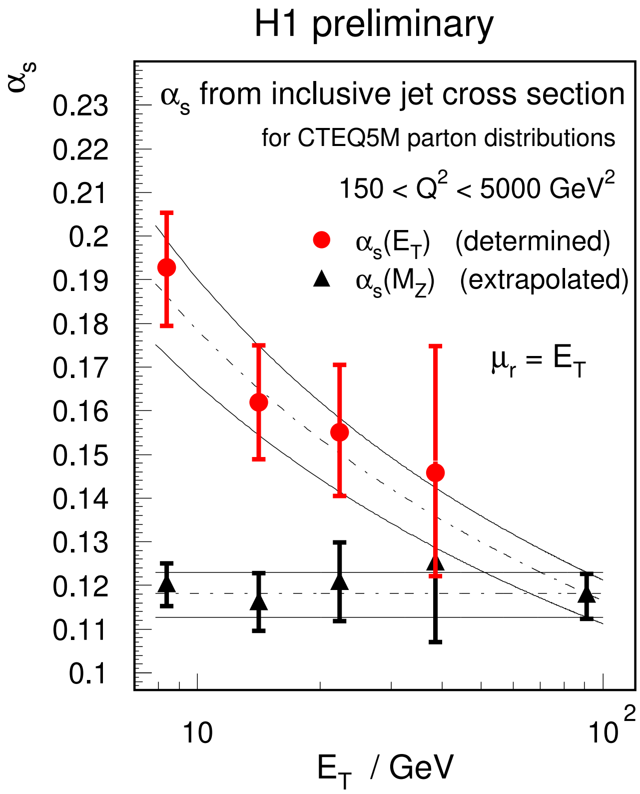

Figure 6: Determination of α_s from the inclusive jet cross section for a renormalization scales $\mu_r = E_T$. The results are shown for each E_T value (circles). The single values are extrapolated to the Z-mass (triangles), and a combined fit gives a result of $\alpha_s(M_Z)$ (rightmost triangle). The upper curves indicate the prediction of the renormalization group equation for the combined fit result and its uncertainty.

6.2 Combined Fit – Central Result

Once we are convinced that our data are consistent over the whole range of Q^2 and E_T we can attempt to make a combined fit. The results of the combined fit are shown in Fig. 6. First of all we perform a fit to the data points of the same E_T (combining the four Q^2 regions) and extract four values of $\alpha_s(E_T)$ (circles). These single values are evolved to $\alpha_s(M_Z)$ (triangles below). A combined fit to all 16 data points leads to the final result of $\alpha_s(M_Z)$ (rightmost triangle). The upper curves in the figure indicate the prediction of the renormalization group equation for the combined result and its uncertainties. The result is:

$$\alpha_s(M_Z) \;=\; 0.1181 \pm 0.0030(\mathrm{exp.})\,^{+0.0039}_{-0.0046}(\mathrm{theo.}) \qquad\qquad (\mu_r = E_T)\,. \tag{3}$$

The uncertainty of this result arising from the uncertainties in the parton distributions is discussed later. The largest contribution to the experimental uncertainty comes from the hadronic energy scale. The theoretical uncertainty is equally distributed between the uncertainty of the hadronization corrections and the renormalization scale uncertainty. The contribution from the renormalization scale uncertainty ($\mu_r = E_T$) is ($^{+0.0025}_{-0.0034}$).

The result (3) is consistent with the current world average value of $\alpha_s = 0.119 \pm 0.004$ [31].

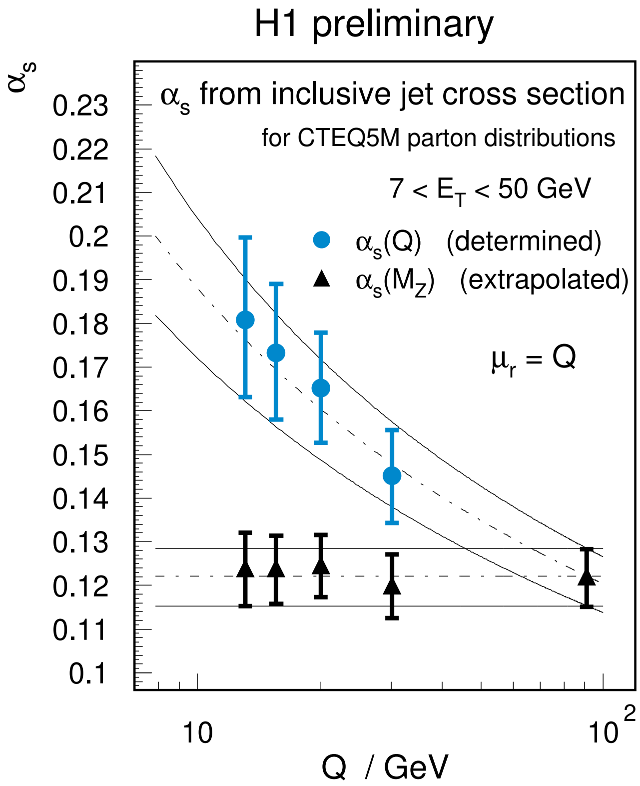

Figure 7: Determination of α_s from the inclusive jet cross section for a renormalization scales $\mu_r = Q$. The results are shown for each Q value (circles). The single values are extrapolated to the Z-mass (triangles), and a combined fit gives a result of $\alpha_s(M_Z)$ (rightmost triangle). The upper curves indicate the prediction of the renormalization group equation for the combined fit result and its uncertainty.

6.3 Choice of a Different Renormalization Scale

Another choice of the renormalization scale in the theoretical calculation could be the four momentum transfer Q. Analog to the procedure used in Fig. 6 we perform an α_s determination for the renormalization scale $\mu_r = Q$. In this case we combine the data of the same Q but different E_T and obtain four single values of $\alpha_s(Q)$ (circles). As done before, we evolve these results to $\alpha_s(M_Z)$ (triangles) and finally perform a combined fit to all data resulting in a combined value of $\alpha_s(M_Z)$ (rightmost triangle). The value is

$$\alpha_s(M_Z) \ = \ 0.1221 \pm 0.0034(\text{exp.})\,^{+0.0054}_{-0.0059}(\text{theo.}) \qquad\qquad (\mu_r = Q)\,. \tag{4}$$

A comparison of this result with the one obtained for $\mu_r = E_T$ in (3) leads to two observations. On one hand the central value is shifted by $+0.0040$. On the other hand we observe a significant increase of the theoretical uncertainty for the choice $\mu_r = Q$. This increase is directly connected to a larger renormalization scale dependence of the perturbative NLO calculation for $\mu_r = Q$, leading to an uncertainty of $\alpha_s(M_Z)$ of ($^{+0.0044}_{-0.0049}$). Within this uncertainty the $\alpha_s(M_Z)$ result is consistent with the one in (3) obtained for $\mu_r = E_T$.

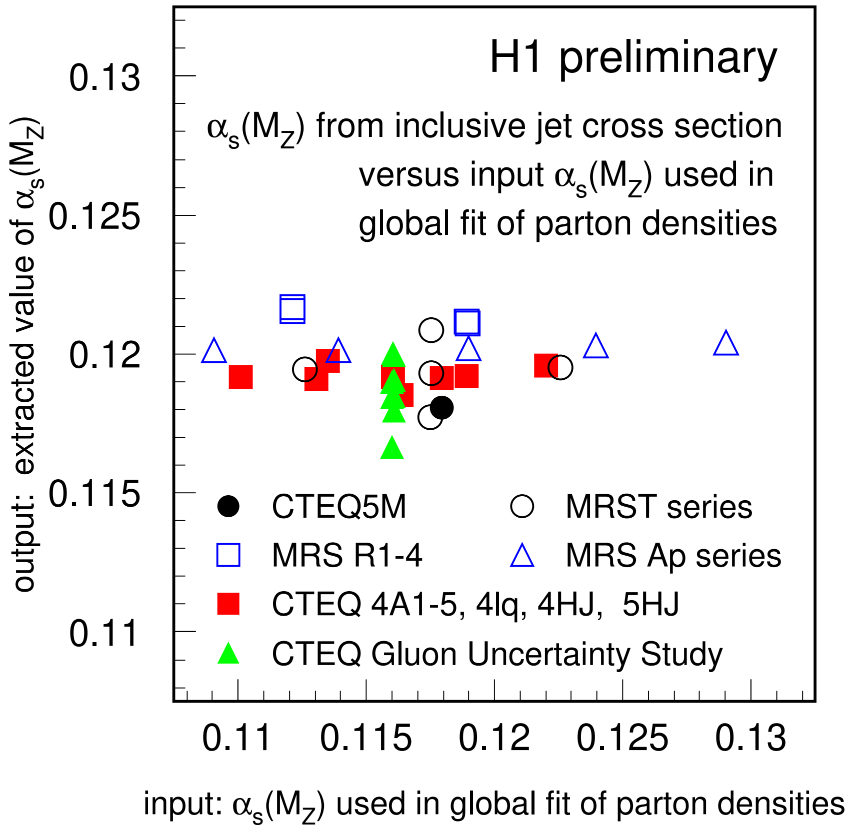

Figure 8: Dependence of the $\alpha_s(M_Z)$ fit result (for $\mu_r = E_T$) on the parton distributions used in the fit. The results are displayed as a function of the $\alpha_s(M_Z)$ value that was used in the global fit of the parton distributions. The correlation is shown for a comprehensive collection of different global fits.

6.4 Variations of Parton Distributions

The assumption of parton distributions which have been determined in other processes and are available from the global fits is the largest limitation of this current approach to determine α_s.

While it is straightforward to propagate the experimental and theoretical uncertainties into the result of α_s, this is not the case for the uncertainties connected to the parton distributions. No global analysis has yet provided an error analysis of the fit results. The uncertainty coming from the parton distributions is usually estimated by comparing fit results from different groups. However, these groups are using nearly the same data sets, and their fits are based on similar assumptions. The spread between these results (which are all “best fits”) does therefore not explore the range of possible variations and does not account for the true uncertainty of the parton distributions. Only the CTEQ Collaboration has performed a study [32] of the uncertainty in the gluon distribution. The global analysis was repeated for different parameterizations of the gluon density, also allowing the quality of the fits to degrade. Only extreme fits were removed that showed clear disagreement with one or more data sets. While this study is a first step towards the estimation of uncertainties, it can still not replace a proper error analysis, needed to determine the uncertainties of parton density functions.

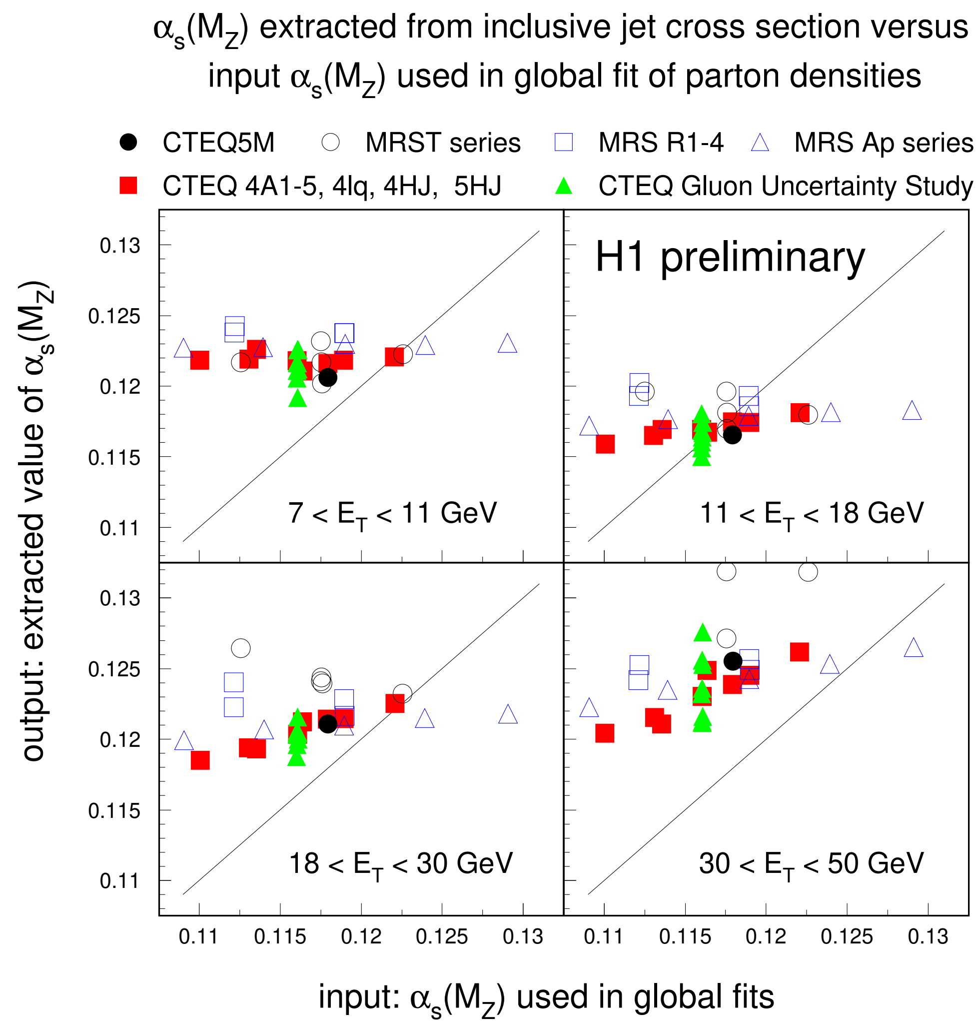

Figure 9: Dependence of the $\alpha_s(M_Z)$ fit result on the $\alpha_s(M_Z)$ value that was used in the global fit of the parton distributions. The correlation is shown separately for each E_T bin.

A second point concerns the question of the consistency of the α_s determination. The parton densities obtained in global fits always depend on an initial assumption of α_s. This may lead to a circular argument in the α_s extraction. Fortunately many recent global fits have provided series of parton distributions for different assumptions of $\alpha_s(M_Z)$ [23, 24, 33]. Using these series of parton distributions, the influence of the initial assumption on $\alpha_s(M_Z)$ can be tested.

Therefore we feel the need to make a detailed study of the dependence of our fit result on these input parameters. We have redone the analysis using nearly all recent parameterizations of parton distributions from global fits, including the CTEQ gluon uncertainty study. The $\alpha_s(M_Z)$ results obtained for the different parton distributions are shown in Fig. 8. The $\alpha_s(M_Z)$ fit results from our inclusive jet data are shown as a function of the $\alpha_s(M_Z)$ value that was used in the global fit. No significant correlation is seen.

The largest deviations to the central result for CTEQ5M parton distributions are obtained for the MRSR3 parameterization and for one of the sets from the CTEQ gluon uncertainty study (for both choices of the renormalization scale). We will quote this whole spread as the uncertainty of our result.

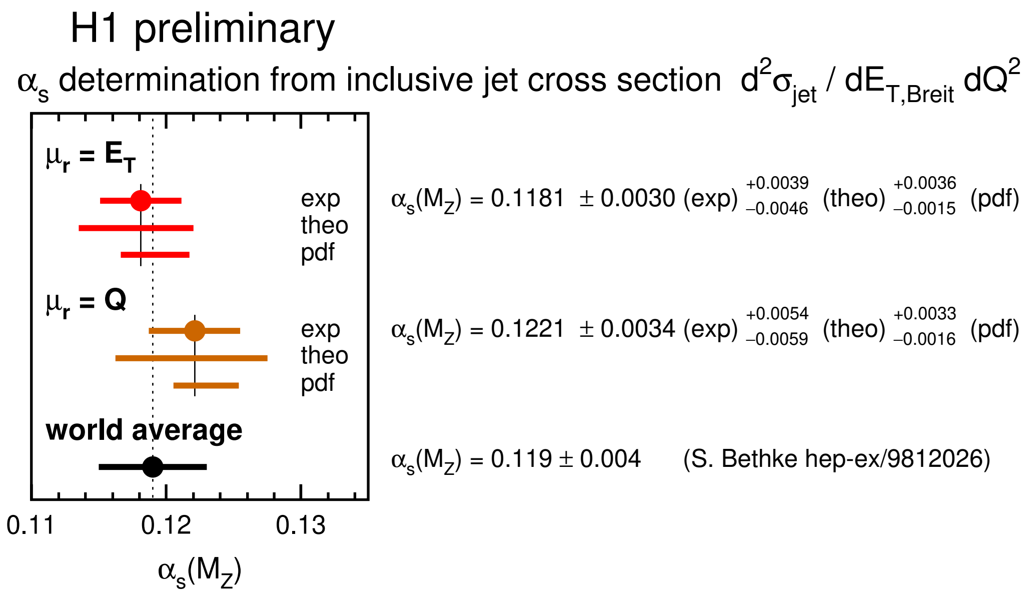

Figure 10: Comparison of the $\alpha_s(M_Z)$ result obtained from the inclusive jet cross section in this analysis for a renormalization scale $\mu_r = E_T$ and $\mu_r = Q$ with the current world average value [31].

The small dependence of our result on the $\alpha_s(M_Z)$ value used in the global fit differs from the observation made by the CDF Collaboration in an α_s analysis of their high E_T inclusive jet cross section [34]. Their $\alpha_s(M_Z)$ result is strongly dependent on the $\alpha_s(M_Z)$ assumption made in the global fits. To investigate the reasons for this difference we also show the correlation plot separately for each E_T bin. For all four $\alpha_s(M_Z)$ values corresponding to each of the four E_T bins in Fig. 6 we have redone the fit for all parton distributions. In Fig. 9 we show the correlation of these results to the $\alpha_s(M_Z)$ value used in the global fits. While for both lower E_T ranges only very small correlations are seen, we see a slightly larger correlation for the bin $18 < E_T < 30\,\mathrm{GeV}$. This effect is increased in the highest E_T bin, where also the absolute spread for parton densities with equal $\alpha_s(M_Z)$ values is larger. However, our data points at high E_T have large statistical uncertainties and less influence on the combined $\alpha_s(M_Z)$ fit results. This is reflected in the small dependence seen in Fig. 8.

The $\alpha_s(M_Z)$ results obtained for a renormalization scale $\mu_r = E_T$ and $\mu_r = Q$ are displayed in Fig. 10 including experimental and theoretical uncertainties and the maximum spread obtained in the variation of the parton density functions. The world average value [31] is shown for comparison.

7 Comparison with an α_s Determination from Dijet Rates

In a recent preliminary analysis [35] we have determined $\alpha_s(M_Z)$ in dijet production. The fraction of dijet events in all deep-inelastic scattering events ("dijet rate") has been measured in the region of four momentum transfers squared $150 < Q^2 < 5000\,\mathrm{GeV}^2$. The analysis has been performed for a different $k_\perp$ jet algorithm [36] in the Breit frame, and for a modified Durham algorithm [37] in the HERA laboratory frame. Values of $\alpha_s(M_Z)$ have been determined [35]

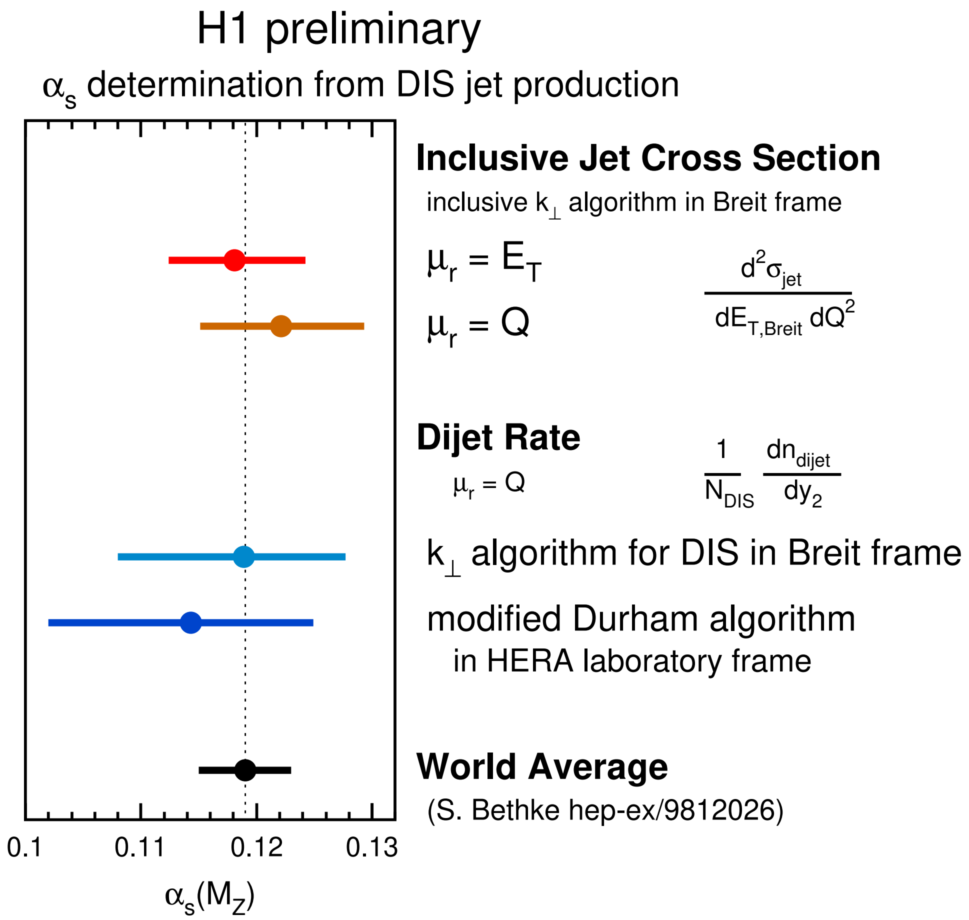

Figure 11: Comparison of the $\alpha_s(M_Z)$ result obtained from the inclusive jet cross section in this analysis (for a renormalization scale $\mu_r = E_T$ and $\mu_r = Q$) with the results fitted to the dijet rate for two different jet algorithms in a recent preliminary H1 analysis [35] (for a renormalization scale $\mu_r = Q$) and with the current world average value [31].

in fits to the distributions of the jet resolution parameter y_2 for both jet algorithms in the range $575 < Q^2 < 5000\,\mathrm{GeV}^2$ using a renormalization scale $\mu_r = Q$. The results from the fit to the dijet rate in the Breit frame using the $k_\perp$ algorithm and to the dijet rate in the HERA laboratory frame using the modified Durham algorithm are shown in Figs. 11 and 12. They are consistent with the results obtained in this paper.

8 Summary

We have presented a measurement of the inclusive jet cross section in the Breit frame in deep-inelastic scattering at large four momentum transfers squared $150 < Q^2 < 5000\,\mathrm{GeV}^2$ and high transverse jet energies $49 < E_T^2 < 2500\,\mathrm{GeV}^2$. For the inclusive $k_\perp$ jet algorithm non-perturbative (hadronization) corrections are seen to be small ($3\% - 10\%$) and perturbative calculations in next-to-leading order in α_s give a good description of the data.

In a QCD fit to these data we have determined the value of the strong coupling constant $\alpha_s(E_T)$ at different values of the renormalization scale $\mu_r = E_T$ in different regions of Q^2.

H1 preliminary

α_s determination from DIS jet production

Inclusive Jet Cross Section $\quad \dfrac{d^2\sigma_{jet}}{dE_{T,Breit}\, dQ^2}$

inclusive $k_\perp$ algorithm in Breit frame

$\mu_r = E_T$

$\alpha_s(M_Z) = 0.1181 \;\pm 0.0030\,(\text{exp})\; ^{+0.0039}_{-0.0046}\,(\text{theo})\; ^{+0.0036}_{-0.0015}\,(\text{pdf})$

$\mu_r = Q$

$\alpha_s(M_Z) = 0.1221 \;\pm 0.0034\,(\text{exp})\; ^{+0.0054}_{-0.0059}\,(\text{theo})\; ^{+0.0033}_{-0.0016}\,(\text{pdf})$

Dijet Rate $\quad \dfrac{1}{N_{DIS}} \dfrac{dn_{dijet}}{dy_2}$

$\mu_r = Q$ $\quad k_\perp$ algorithm for DIS in Breit frame

$\alpha_s(M_Z) = 0.1189 \; ^{+0.0064}_{-0.0081}\,(\text{exp})\; ^{+0.0059}_{-0.0046}\,(\text{theo})\; ^{+0.0013}_{-0.0055}\,(\text{pdf})$

$\mu_r = Q$ $\quad$ modified Durham algorithm in laboratory frame

$\alpha_s(M_Z) = 0.1143 \; ^{+0.0075}_{-0.0089}\,(\text{exp})\; ^{+0.0074}_{-0.0064}\,(\text{theo})\; ^{+0.0008}_{-0.0054}\,(\text{pdf})$

World Average

$\alpha_s(M_Z) = 0.119 \pm 0.004$ $\quad$ (S. Bethke hep-ex/9812026)

Figure 12: Comparison of the $\alpha_s(M_Z)$ result obtained from the inclusive jet cross section in this analysis (for a renormalization scale $\mu_r = E_T$ and $\mu_r = Q$) with the results fitted to the dijet rate for two different jet algorithms in a recent preliminary H1 analysis [35] (for a renormalization scale $\mu_r = Q$) and with the current world average value [31].

The single results are evolved to M_Z using the 4-loop formula and are consistent over the whole phase space considered here. In a combined fit to all data we have extracted the value of $\alpha_s(M_Z)$. While using the CTEQ5M parton densities for the central result we have repeated the analysis using various other parton distributions from different global fits. The combined result of our analysis (obtained for $\mu_r = E_T$) is

$$\alpha_s(M_Z) \;=\; 0.1181 \pm 0.0030(\text{exp.})\,^{+0.0039}_{-0.0046}(\text{theo.})\,^{+0.0036}_{-0.0015}(\text{pdf}) \qquad (\mu_r = E_T)\,.$$

We have also studied the use of a renormalization scale $\mu_r = Q$ and obtain the result

$$\alpha_s(M_Z) \;=\; 0.1221 \pm 0.0034(\text{exp.})\,^{+0.0054}_{-0.0059}(\text{theo.})\,^{+0.0033}_{-0.0016}(\text{pdf}) \qquad (\mu_r = Q)\,.$$

While for $\mu_r = Q$ the $\alpha_s(M_Z)$ result is higher by $+0.0040$, the uncertainty connected to the renormalization scale dependence is increased to $^{+0.0044}_{-0.0049}$ (compared to $^{+0.0025}_{-0.0034}$ for $\mu_r = E_T$). Within the larger uncertainty for the scale $\mu_r = Q$ both results are compatible. The $\alpha_s(M_Z)$ result obtained in this analysis is consistent with the current world average value of $\alpha_s = 0.119 \pm 0.004$ [31].

References

[1] S.D. Ellis and D.E. Soper, Phys. Rev. D 48 (1993) 3160.

[2] S. Catani, Yu.L. Dokshitzer, M.H. Seymour and B.R. Webber, Nucl. Phys. B 406 (1993) 187.

[3] M. Wobisch and T. Wengler, to appear in: Proceedings of the Workshop on Monte Carlo Generators for HERA Physics, eds. G. Grindhammer, G. Ingelman, H. Jung, T. Doyle, DESY (1999).

[4] JADE Collab., W. Bartel et al., Z. Phys. C33 (1986) 23.

[5] D. Graudenz and N.Magnussen, Proceedings of the Workshop Physics at HERA, Vol. 1, eds. W. Buchmüller and G. Ingelman, DESY (1991) 261.

[6] H1 Collab., C. Adloff et al., Eur. Phys. J. C6 (1999) 575.

[7] H1 Collab., C. Adloff et al., Eur. Phys. J. C 5 (1998) 625.

[8] H1 Collab., I. Abt et al., Nucl. Instr. and Meth. A 386 (1997) 310 and 348.

[9] H1 Collab., C. Adloff et al., Measurement of Neutral and Charged Current Cross-Sections in Positron-Proton Collisions at Large Momentum Transfer, in preparation.

[10] U. Bassler and G. Bernardi, Nucl. Instr. Meth. A 426 (1998) 583.

[11] S. Bentvelsen, J. Engelena and P. Kooijman, Proceedings of the Workshop Physics at HERA, eds. W. Buchmüller, G. Ingelman, DESY (1991).

[12] U. Bassler and G. Bernardi, Nucl. Instr. Meth. A 361 (1995) 197.

[13] G. Ingelman, A. Edin and J. Rathsman, Comp. Phys. Comm. 101 (1997) 108, Version used: 6.5.

[14] L. Lönnblad, Comp. Phys. Comm. 71 (1992) 15, Version used: 4.08.

[15] K. Charchula, G. Schuler and H. Spiesberger, Comp. Phys. Comm. 81 (1994) 381.

[16] S. Catani and M.H. Seymour, Nucl. Phys. B 485 (1997) 291, Erratum-ibid. B 510 (1997) 503.

[17] CTEQ Collab., H.L. Lai et al., hep-ph/9903282.

[18] B.R. Webber, Nucl. Phys. B 238 (1984) 492.

[19] B. Andersson et al., Phys. Rep. 97 (1983) 31.

[20] T. Sjöstrand, Comp. Phys. Comm. 39 (1986) 347; T. Sjöstrand and M. Bengtsson, ibid. 43 (1987) 367.

[21] G. Marchesini et al., Comp. Phys. Comm. 67 (1992) 465, version used: 5.9.

[22] E.B. Zijlstra and W.L. van Neerven , Nucl. Phys. B 383 (1992) 525.

[23] CTEQ Collab., H.L. Lai et al., Phys. Rev. D 55 (1997) 1280.

[24] A.D. Martin, R.G. Roberts, W.J. Stirling and R.S. Thorne, Eur. Phys. J. C 4 (1998) 463.

[25] T. van Ritbergen et al., Phys. Lett. B 400 (1997) 379.

[26] K.G. Chetyrkin et al., Phys. Rev. Lett. 79 (1997) 2184.

[27] M. Wobisch, PhD thesis, Aachen, in preparation.

[28] G. Lobo, Proceedings of the Workshop Future Physics at HERA, eds. G. Ingelman, A. De Roeck and R. Klanner, DESY (1996) 537.

[29] F. James and M. Roos, Comp. Phys. Comm. 10 (1975) 343.

[30] F. Zomer, Proceedings of the Workshop on Deep-Inelastic Scattering and QCD (DIS97), eds. D. Krakauer and J. Repond, Chicago, Illinois (1997).

[31] S. Bethke, in Proceedings of: 4th International Symposium on Radiative Corrections (RADCOR 98), Catalonia, Spain, (1998) hep-ex/9812026.

[32] J. Huston et al., Phys. Rev. D 58 (1998) 114034.

[33] A.D. Martin, W.J. Stirling, R.G. Roberts, Phys. Lett. B 356 (1995) 89.

[34] A. Akopian, Proceedings of 7th International Workshop on Deep Inelastic Scattering and QCD (DIS 99), Zeuthen, Germany (1999).

[35] H1 Collab., Study of differential Di-Jet Event Distributions and Determination of α_s in Deep-Inelastic Scattering at large Q^2, abstract 157 submitted to this conference.

[36] S. Catani, Yu.L. Dokshitzer and B.R. Webber, Phys. Lett. B 285 (1992) 291.

[37] N. Tobien, PhD thesis, Hamburg, in preparation.